Study of Contact Ion Pairs of Supersaturated Magnesium Sulfate Solutions Using Raman Scattering of Levitated Single Droplets

Yun-Hong Zhang[†] and Chak K. Chan*[,‡]

College of Chemical Engineering & Materials Science, Beijing Institute of Technology, Beijing 100081, China, and Department of Chemical Engineering, The Hong Kong University of Science and Technology, Hong Kong, China

Received: April 10, 2000; In Final Form: July 14, 2000

Significant retardation of the evaporation rate of levitated aqueous $MgSO_4$ droplets has been found at high concentrations using an electrodynamic balance. Raman spectroscopy was used to study the structural changes, in particular, the formation of contact ion pairs, in supersaturated aqueous $MgSO_4$ droplets at ambient temperatures. As the relative humidity (RH) decreases, single levitated droplets lose water and become supersaturated. A molar water-to-solute ratio as low as 1.54 was obtained, facilitating the study of contact ion pairs of unhydrated Mg^{2+} and SO_4^{2-} ions in $MgSO_4$ solutions. The characteristics of the ν_1-SO_4^{2-} band change as a function of the water-to-solute ratio. Overall, a frequency shift from 983 to 1007 cm^{-1} and an increase of the full width at half-height from 12 to 54 cm^{-1} of the ν_1-SO_4^{2-} band were observed when the water-to-solute molar ratio decreased from 17.29 to 1.54. Most of the changes occur at a ratio smaller than 6, instead of at the saturation ratio of 15.60. These changes are attributed to the formation of contact ion pairs with different structures. A chain structure based on the contact ion pair of bidentate was proposed. Formation of close contact ion pairs and chain structures can explain the retardation of evaporation of supersaturated $MgSO_4$ droplets observed in previous experiments. On the basis of the comparisons of the Raman spectra of $MgSO_4$ and $(NH_4)_2SO_4$, we assigned the shoulder appearing at 995 cm^{-1} in bulk $MgSO_4$ studies to the contact ion pairs instead of the solvent-separated ion pairs.

Introduction

The hygroscopic properties of atmospheric aerosols affect air quality, visibility, and global climate. Depending on the ambient relative humidity and chemical compositions, atmospheric aerosols will attain an appropriate amount of water. If the aerosol composition is fixed, the typical characteristic time for growth or shrinking of an aerosol as a result of gas−aerosol water transport is orders of magnitude less than 1 s.[1] Hence, equilibrium is usually assumed in the modeling and field studies of hygroscopic properties of atmospheric aerosols. Mass transfer in achieving gas−aerosol equilibrium of semi-volatile species such as ammonium can take a much longer time.[2,3] Although coatings of hydrophobic materials on inorganic aerosols have been found to retard the hygroscopic growth and shrinking of aqueous inorganic aerosols,[4−6] atmospheric aerosols are in general expected to respond to changes of RH almost instantaneously in most applications.

Recently, Chan et al.[7] studied the evaporation of singly levitated solution droplets of ceramic precursor including $MgSO_4$ and $MgCl_2$ in an electrodynamic balance (EDB). In their study, droplets initially equilibrated at RH = 85% were dried by nitrogen at 20−50 mL min^{-1} at ambient temperatures. As shown in Figure 1, aqueous $MgCl_2$ droplets effloresce at low RH but $MgSO_4$ droplets do not. More importantly, $MgSO_4$ droplets exhibit a significant reduction in the evaporation rate after a transition at about 1.2 h, suggesting that mass transfer limitations are important at high concentrations. The long duration of evaporation is due to the small flow rate of nitrogen and the relatively large dead volume of the chamber they used to contain the EDB. Chan et al.[8] also observed mass transfer limitations in the evaporation of equimolar $Na_2SO_4/MgSO_4$ solutions but not of mixed solutions of NaCl−$MgCl_2$, NaCl−$Mg(NO_3)_2$, and NaCl−$MgSO_4$. Chan and co-workers[7,8] proposed that the $MgSO_4$ solutions form a gel at high concentrations, leading to a significant increase in the diffusional resistance in the droplet. Although they did not study the molecular structures of concentrated $MgSO_4$ solutions, it is apparent that concentrated $MgSO_4$ solutions have structural characteristics different from dilute solutions.

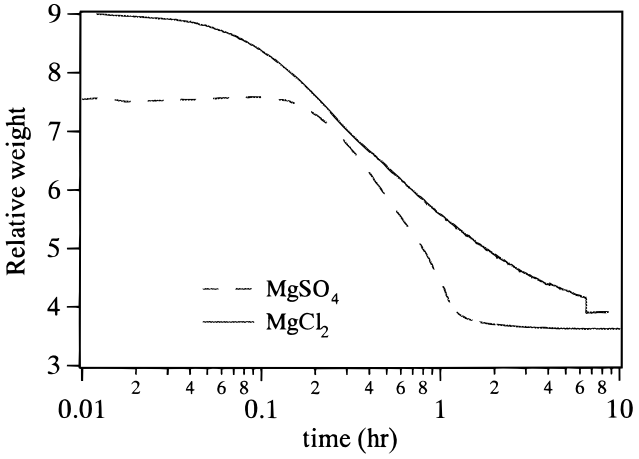

Figure 1. Evaporation of water from supersaturated $MgSO_4$ and $MgCl_2$ droplets.

* Corresponding Author. E-mail: keckchan@ust.hk.
[†] Beijing Institute of Technology. E-mail: yhz@bit.edu.cn.
[‡] The Hong Kong University of Science and Technology.

10.1021/jp0013659 CCC: $19.00
Published on Web 09/14/2000

Many studies of the ion association in aqueous solutions in the $MgSO_4-H_2O$ system using classical methods such as freezing point measurements,[9] potentiometric measurements,[10] ultrasonic absorption,[11,12] and solubility measurements[13] have been reported. In general, there are two types of ion association in aqueous electrolyte solutions. The first type is the strong association complex (contact ion pair) of cations and anions forming a covalent bond. The residence time of the contact ion pair is sufficiently long so that the pair can be considered as an individual chemical component of a fixed stoichiometric composition. Thus it is possible to detect the contact ion pairs directly by spectroscopic methods. The second type is the weak association complex in the form of solvent-separated ion pairs, associated by predominantly electrostatic forces. The composition of the solvent-separated ion pairs changes with the ionic strength of the solution. Although the contact ion pairs may be stochastically formed from collision between the cations and anions, they are easily perturbed by hydration and are therefore difficult to detect. Atkinson and Pstriucci suggested that the following processes occur in aqueous $MgSO_4$ solutions:[12]

$$Mg^{2+}(aq) + SO_4^{2-}(aq) = [Mg(WW)SO_4] \rightleftharpoons [Mg(W)SO_4] \rightleftharpoons [MgSO_4]$$

Here, $Mg^{2+}(aq)$ and $SO_4^{2-}(aq)$ represent the free hydrated ions. $[Mg(WW)SO_4]$ and $[Mg(W)SO_4]$ represent the ion pairs separated by two and one water molecules, respectively. $[MgSO_4]$ represents the contact ion pair.

Raman spectroscopy has been used to study the formation of the contact ion pair $[MgSO_4]$ (inner-sphere structure) and the solvent-separated ion pairs $[Mg(WW)SO_4]$ and $[Mg(W)SO_4]$ (outer-sphere structure). To date, there is still no agreement on the existence of the contact ion pair in aqueous $MgSO_4$ solutions. Davis and co-workers resolved two bands at 982 (half-width 14 cm^{-1}) and 995 cm^{-1} (half-width 25 cm^{-1}), using the slight asymmetry of the high-frequency side of the ν_1-SO_4^{2-} band.[14−15] Such asymmetry has also been observed in sulfate solutions of Li^+, Al^{3+}, Fe^{2+}, Cd^{2+} and attributed to the existence of contact ion pairs in an inner-sphere structure.[16−23] On the other hand, Daly et al.[24] did not observe any Raman signature related to the formation of ion pairs in $MgSO_4$ aqueous solutions. They proposed that $MgSO_4$ ion pairs in solutions should be of an outer-sphere or solvent-separated structure, which cannot affect the Raman spectrum of SO_4^{2-}. Similar conclusions were reached by Rull et al.[25] in their study of $MgSO_4$ solutions of concentrations of 0.5−2.8 mol L^{-1} at 5−80 °C.

One of the difficulties in detecting the contact ion pairs is their short life span in dilute or even saturated solutions. To detect the contact ion pairs, if they exist, there should be insufficient water molecules in the solution so that a saturated hydrated-inner-sphere cannot be formed. Such a low water-to-solute environment can be found in supersaturated solutions. The electrodynamic balance (EDB) has been demonstrated to be a very useful tool for studying levitated single particles of supersaturated solutions.[26] Since the droplets are freely levitated in an electric field, heterogeneous nucleation is suppressed. Many thermodynamic studies of supersaturated solutions of inorganic salts using an EDB have been reported.[27−30] Furthermore, combining the EDB with a Raman spectroscopic system, Tang et al.[27,28] studied the phase transformation and metastability of supersaturated microparticles. Others have used Raman spectroscopy to investigate transport properties and chemical reactions of suspended aerosols.[31−33] Schweiger[34] recently reviewed the application of Raman spectroscopy on aerosol particles.

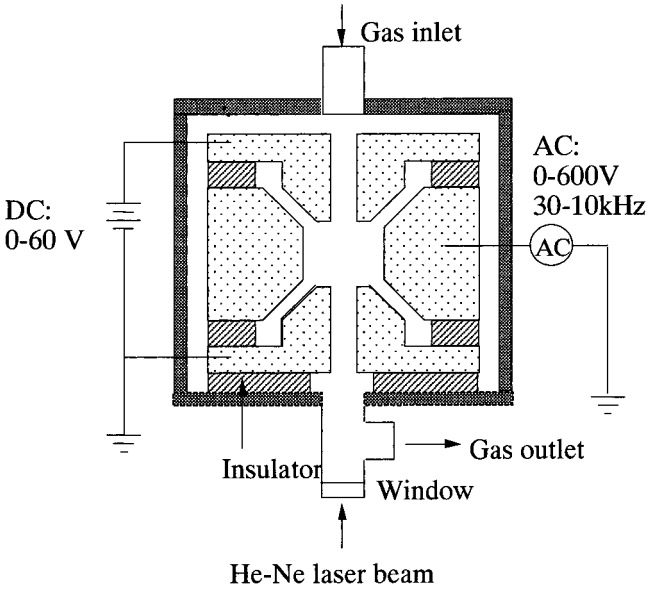

Figure 2. The electrodynamic balance for studying single supersaturated droplets.

In this paper we report the Raman spectra and the observation of the contact ion pair between Mg^{2+} and SO_4^{2-} in supersaturated $MgSO_4$ solutions using an EDB. The spectra are compared with those of an $(NH_4)_2SO_4$ solution, which has been considered to be a model of free sulfates.[21−23]

Experimental Section

The development and applications of the electrodynamic balance (EDB) have been reviewed in detail by Davis.[26] Figure 2 shows the design of the EDB used in this study. It consists of a pair of DC endcap electrodes and an AC ring electrode. Droplets of dilute solutions were ejected by a piezoelectric particle generator (Uni-Photon-Inc., model 201) and were charged by induction before they entered the EDB. A single charged droplet was then trapped in the EDB. In particular, the electrostatic force imposed on the particle by the DC voltage balances the weight of the particle and keeps the particle stationary at the center of the EDB. Hence, the mass of a droplet is proportional to the DC balancing voltage. When a droplet is equilibrated with the surrounding environment inside the EBD, the water activity (a_w) of the droplet is related to the relative humidity (RH) by $a_w = P_w/P_w^{sat} = RH/100$. In the above equation, P_w is the partial pressure of water of the ambient environment and P_w^{sat} is the saturation water vapor pressure at the ambient temperature T. The Kelvin effect to correct for vapor pressure dependence of curvature of a droplet can be ignored since the particles are in the order of 30 μm in diameter. The water-to-solute molar ratio of the droplet was changed by altering the ambient RH and was determined by the DC balancing voltage measurements. Since the EDB used in this study has a much smaller residence time than the one used by Chan et al.,[7] particles were equilibrated at each RH within an hour. The air flow for controlling RH in the EDB was momentarily stopped when the balancing voltage was measured. The RH was determined by a dew-point hygrometer (EG&G DewPrime model 2000).

A Raman system, consisting of a 5 W argon ion laser (Coherent I90-5) and a 0.5 m monochromator (Acton SpectraPro500) attached with a CCD (Princeton Instrument, TE/CCD-1100PFUV) detector, was incorporated into the EDB system. The 514.5 nm line of an argon-ion laser with power between 1 and 1.4 W was used as the source of excitation. A pair of lenses,

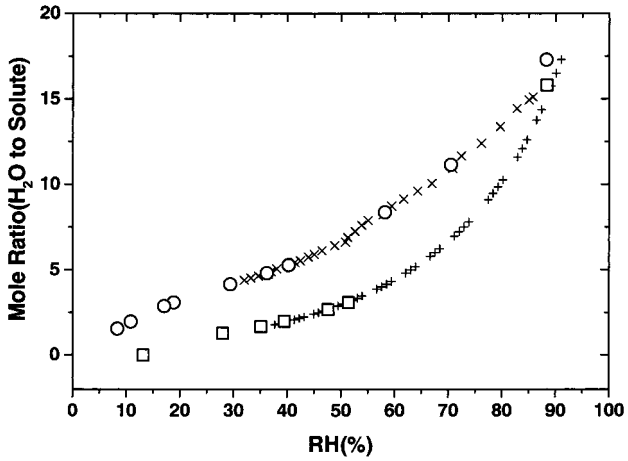

Figure 3. Water activity data of $MgSO_4$ and $(NH_4)_2SO_4$: Circles, $MgSO_4$ measurements; crosses, $MgSO_4$ data from Ha and Chan;[22] squares, $(NH_4)_2SO_4$ measurements; plus signs, $(NH_4)_2SO_4$ data from Tang et al.[19]

which matches the *f*/7 optics of the monochromator, was used to focus the 90° scattering of the levitated droplet on the slit of the monochromator. A 514.5 nm Raman notch filter was placed between the two lenses to remove the strong Rayleigh scattering. A 1200 g/mm grating of the monochromator was selected. The resolution of the spectra obtained is 2.3 cm^{-1} at 981 cm^{-1}. All measurements were made at ambient temperatures of 22−24 °C. The integration time of each spectrum was 40 s. Typically, five spectra were averaged to produce a spectrum at each RH.

Results

1. Compositional Dependence of Aqueous $MgSO_4$ and $(NH_4)_2SO_4$ Droplets on Relative Humidity. To relate the Raman spectra to the molar water-to-solute ratio of the supersaturated droplets, the compositional dependence of the droplet on RH was determined. Figure 3 shows the molar water-to-solute ratio of $MgSO_4$ and $(NH_4)_2SO_4$ solutions as a function of RH. These measurements were made when RH was decreased in steps. Our measurements of $MgSO_4$ (the open circles) are in good agreement with the data of Ha and Chan[30] (the crosses). Furthermore, we have extended the measurements to RH = 8.3% where the water-to-solute ratio is only 1.54. It should be noted that $MgSO_4$ does not form an anhydrous salt even at RH = 8.3%. The measurements of $(NH_4)_2SO_4$ (the open squares) also agree well with those of Tang et al.[27] (the plus signs) at 25 °C. In our measurements, $(NH_4)_2SO_4$ achieves a water-to-solute ratio of 1.28 at RH = 28% before it crystallizes to form an anhydrous salt at RH = 13%.

2. Raman Spectra of Aqueous $MgSO_4$ and $(NH_4)_2SO_4$ Droplets. *2.1 Dilute Droplets*. Free SO_4^{2-} ions have T_d symmetry and nine modes of internal vibration spanning the representation $\Gamma_{vib} = A_1 + E + 2F_2$. All modes are Raman active but only the F_2 modes are IR active. Figure 4 shows the Raman spectra of a dilute $(NH_4)_2SO_4$ solution droplet at RH = 88.4% (H_2O to solute ratio = 15.80) and a dilute $MgSO_4$ solution droplet at RH = 88.3% (H_2O to solute ratio = 17.29). Four Raman bands, assigned to the bending modes ν_2 with symmetry of E and ν_3 with symmetry of F_2, and the totally symmetric stretching mode ν_1 (A_1) and the anti-symmetric stretching mode $\nu_4(F_2)$ of the SO_4^{2-} ion at ∼458, ∼618, 983, and ∼1126 cm^{-1}, respectively, are clearly discernible. As shown in the bottom spectrum of the insert in Figure 4, the ν_1-SO_4^{2-} band of $MgSO_4$ solutions is asymmetric with a shoulder at about

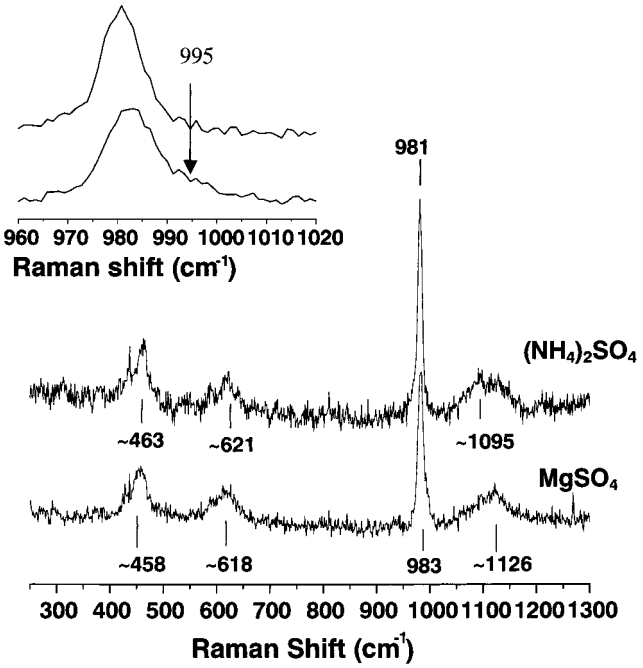

Figure 4. The Raman spectra of droplets $(NH_4)_2SO_4$ with a water-to-salt ratio of 15.8 and $MgSO_4$ with a water-to-salt ratio of 17.3. Insert: The asymmetry of the ν_1-SO_4^{2-} band: $(NH_4)_2SO_4$, top spectrum; $MgSO_4$, bottom spectrum.

995 cm^{-1}. This observation was also found in the spectrum of the bulk solutions reported in the literature.[14] In contrast, the ν_1-SO_4^{2-} band of the $(NH_4)_2SO_4$ solution droplet at 981 cm^{-1} is symmetric (top spectrum of the insert), as reported in the literature for bulk solutions of similar concentrations.[21] The hexaaquo Mg(II) band at 354 cm^{-1} of the $MgSO_4$ droplet was not detected because of the low signal-to-noise ratio and low intensity of this peak.[16]

2.2 Supersaturated Droplets. Figure 5a,b shows the Raman spectra of droplets of $MgSO_4$ and $(NH_4)_2SO_4$ solutions, respectively, at various water-to-solute ratios. The most distinct difference between the spectra of the two species is the change of the peak position and the full width at half-height (fwhh) of the ν_1-SO_4^{2-} band at highly supersaturated concentrations. Figure 6 shows the peak position and the fwhh of $MgSO_4$ and $(NH_4)_2SO_4$ as a function of the water-to-solute ratio. The strongest band of the $MgSO_4$ droplet, ν_1-SO_4^{2-} (including the SO_4^{2-} ion-related bands), has an overall blue-shift from 983 to 1007 cm^{-1} and an increase of its fwhh from 12 to 54 cm^{-1} when the ratio decreases from 17.29 to 1.54 (and RH decreases from 88.3% to 8.4%). The spectral changes can be roughly divided into two steps. From the ratio of 17 to 8, the spectral response is not sensitive to the ratio even though the solutions with ratios smaller than 15.6 are already supersaturated. The peak position of the ν_1-SO_4^{2-} band shifts slightly from 983 to 984 cm^{-1}, and the fwhh increases from 12 to 15 cm^{-1}. However, the spectral response is a very sensitive function of the ratio between 8 and 1.54. The ν_1-SO_4^{2-} band continues its blue-shift to 990 cm^{-1} and its increase of the fwhh to 19 cm^{-1} when the ratio reaches 5. As the ratio decreases further, both the peak position and the fwhh undergo abrupt changes. Finally, the ν_1-SO_4^{2-} band appears at 1007 cm^{-1} as a rotund envelope at ratio =1.54.

In contrast, the ν_1-SO_4^{2-} band of $(NH_4)_2SO_4$ has little spectral change as the water-to-solute ratio varies. The peak position has a little red-shift from 981 to 977 cm^{-1}, and its fwhh increases slightly from 9 to 12 cm^{-1} when the ratio changes from 15.80

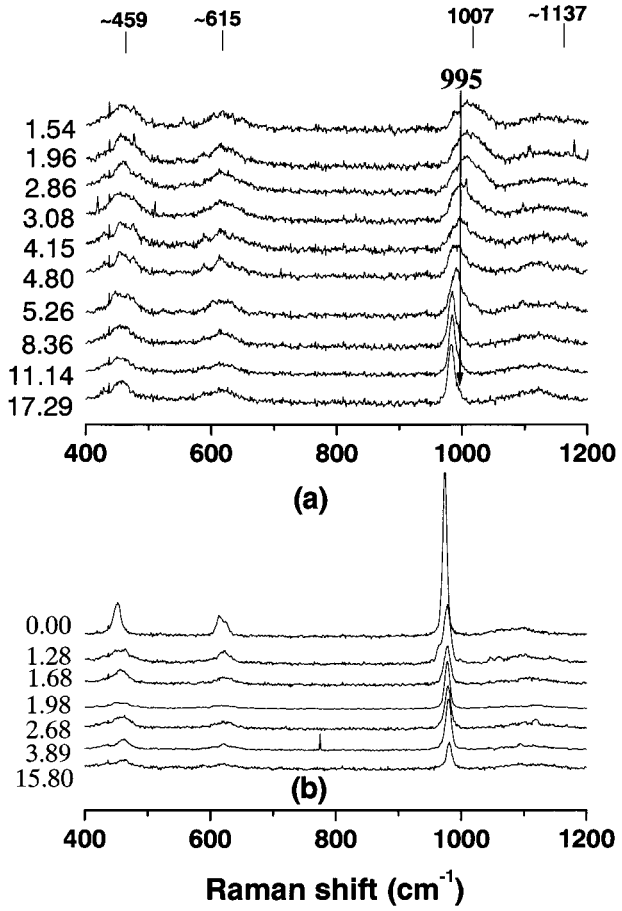

Figure 5. The Raman spectra of droplets (a) $MgSO_4$ and (b) $(NH_4)_2SO_4$ at different water-to-solute mole ratios.

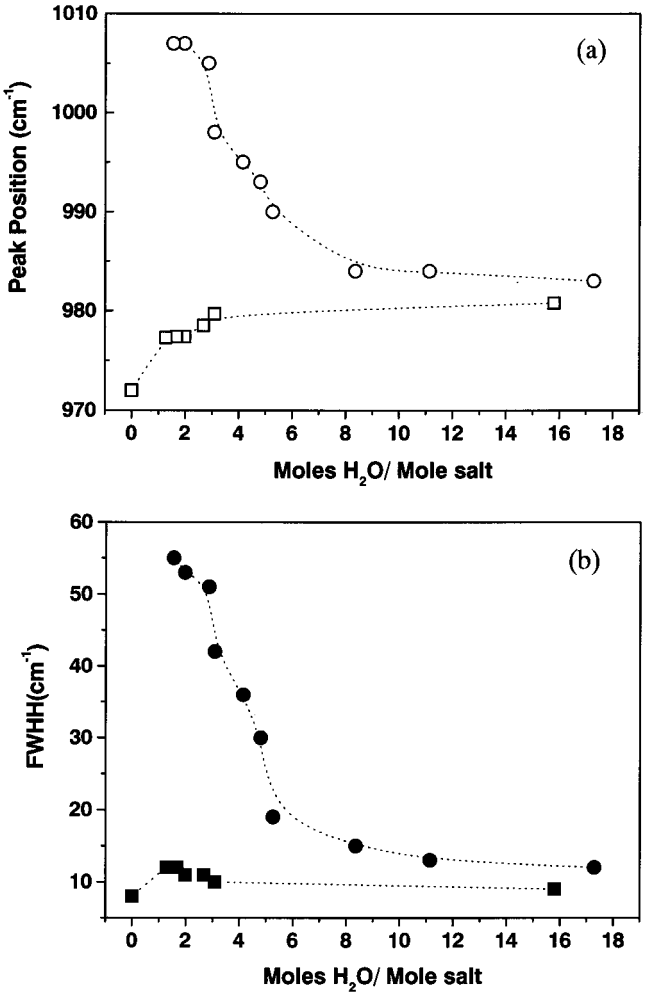

Figure 6. The dependence of (a) the peak position and (b) fwhh of the ν_1-SO_4^{2-} band on the water-to-salt ratio. Open circles, peak positions of $MgSO_4$ spectra; solid circles, fwhh of $MgSO_4$ spectra; open squares, peak positions of $(NH_4)_2SO_4$ spectra; solid squares, fwhh of $(NH_4)_2SO_4$ spectra.

to 1.28. This band shifts to 973 cm^{-1} with an abrupt increase in intensity at RH = 11.3% when crystallization occurs to form an anhydrous particle. The fwhh also decreases to 8 cm^{-1}.

Discussion

Raman spectra are sensitive not only to the strong interaction between adjoining atoms in a covalent bond but also to the weak intermolecular forces including hydrogen bonding and van der Waals force that act over long distances. It has been extensively observed that the ν_1-SO_4^{2-} band is sensitive to the microenvironment of the sulfate ions.[14−25] To date, however, there is no agreement on the relationship between the contact ion pairs and the characteristics of the ν_1-SO_4^{2-} band in dilute solutions. For example, Nomura et al.[35] attributed the asymmetry of the ν_1-SO_4^{2-} band in Li_2SO_4, $MgSO_4$, and $In_2(SO_4)_3$ solutions to the change of the rotational correlation time of water near the sulfate ion and the cation but not to the formation of contact ion pairs. Hayes et al.[36] ascribed the change of the band position to the change of the local potential field experienced by the sulfate ion in the presence of the counterion. Rull et al.[25] suggested that Raman spectroscopy can detect only the association complexes in which the SO_4^{2-} anions are asymmetrically perturbed by the electrostatic interactions with the metal ions directly or through the hydration water molecules in the first coordination sphere, but cannot detect contact ion pairs. Rull et al.[37] studied the Raman spectra of 1 M $MgSO_4$ solutions at high pressures and temperatures and partially dehydrated solid samples formed at different temperatures. They found that the shoulder of 990 cm^{-1} at temperatures below 100 °C changed to a peak at temperatures over 144 °C. They explained this change by the solvent-separated ion association although they also suggested the presence of "more close interactions than the solvent-separated ones" at 206 °C. Other researchers used the shoulder peak at 995 cm^{-1} as an indicator of the presence of the contact ion pair in many quantitative Raman studies.[14,16,21−23]

In our experiments, the lowest water-to-solute ratios attained in the supersaturated droplets of $MgSO_4$ and $(NH_4)_2SO_4$ are 1.54 and 1.38, respectively. Direct interaction between the ions is strong at such small ratios. The strong dependence of the peak position and the fwhh on the ratio of $MgSO_4$ solutions shown in Figures 5 and 6 is an indication of the formation of the contact ion pairs between Mg^{2+} ions and SO_4^{2-} ions. Furthermore, the increase of the intensity of the high-frequency wing of the ν_1-SO_4^{2-} band as the ratio decreases also supports the formation of the contact ion pairs. The broadening of the band is the result of the distribution of contact ion pairs with different structures. Figure 7 shows some proposed structural units of contact pairs of SO_4^{2-} and Mg^{2+} to form monodentate, bidentate, and bridge-bidentate complexes, which have been observed in some sulfate crystals.[38−42] The formation of a chain structure of the contact ion pairs can explain the reduction in the evaporation rate in concentrated $MgSO_4$ droplets observed by Chan et al..[7] A proposed chain structure of $MgSO_4$ based on the structural unit of bidentate is shown in Figure 7.

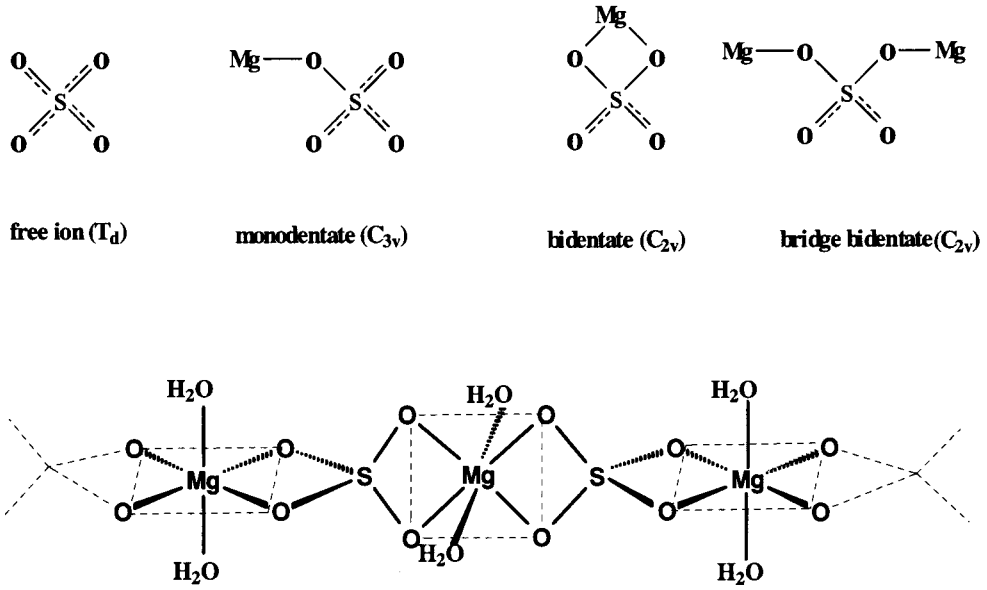

Figure 7. The proposed structural units of contact pairs of Mg^{2+} and SO_4^{2-} of monodentate, bidentate, and bridge-bidentate complexes and a chain structure of bidentate with the $H_2O/MgSO_4$ ratio of 2:1.

Magnesium is an alkali earth metal element in the third period. Having a large charge-to-radius ratio, Mg^{2+} has a tendency to be hydrated instead of polarized in solutions. Both proton NMR in 3−4 mol L^{-1} aqueous perchlorate at a low temperature (−70 °C)[43] and X-ray diffraction[44] studies have confirmed that there are six water molecules in the inner sphere of hydrated Mg^{2+} ions with an internuclear Mg−O distance of 0.211 nm. Pye et al.[16] have given the optimized geometry of the hexaaquo Mg^{2+} complex with T_h symmetry by ab initio method, and they calculated the vibrational frequencies of such a structure. The SO_4^{2-} ions are known to form hydrogen bonds with water molecules and are considered to be "structure maker" ions.[45] Hence, both Mg^{2+} and SO_4^{2-} are highly hydrated in dilute aqueous solutions.

In Figure 5, the Raman spectrum only starts to change at RH = 58.2% (with water-to-solute ratio of 8), instead of at the saturation point of $MgSO_4$ (at RH = 86% at 25 °C). At the ratio of 8, Mg^{2+} ions maintain the hexaaquo Mg^{2+} structure with the other two water molecules linking the first full-layer of the hydrated Mg^{2+} ions and sulfate ions. In this case, the solven-separated ion pairs, i.e., [Mg(W)SO_4] and [Mg(WW)-SO_4], are the main components in the solution. No peak at 995 cm^{-1} was observed at this ratio. As the ratio further decreases to 4.80 and 3.08, the shoulder intensity increases and the shoulder becomes a peak. These observations at ratios smaller than 6 suggest that the shoulder at 995 cm^{-1}, which has been extensively discussed in dilute solutions, corresponds to contact ion pairs instead of solvent-separated ion pairs. In other words, the shoulder at 995 cm^{-1} of the ν_1-SO_4^{2-} band should be related to the interaction of sulfate ions with the inner incomplete hydrated layer of Mg^{2+} ions. Rull et al.[37] measured the Raman spectra of various solid hydrates of $MgSO_4$ formed at different temperatures and found that ν_1-SO_4^{2-} band shifts from 985 to 1001 cm^{-1} when $MgSO_4 \cdot 7H_2O$ is changed to $MgSO_4 \cdot 6H_2O$. However, little change of the fwhh was observed. Their measurements of solid hydrates formed at high temperatures may not be directly compared with our measurements of supersaturated solutions at ambient conditions.

Compared with Mg^{2+} ions, NH_4^+ has a low charge-to-radius ratio. Its partial molar ionic volume is 18 cm^3 mol^{-1} at 25 °C and has a less electrostrictive effect on water than Mg^{2+} has. Thus, sulfate ions exist as free ions in bulk $(NH_4)_2SO_4$ solutions.[20] Hence, the ν_1-SO_4^{2-} band characteristics of the $(NH_4)_2SO_4$ solution droplet is not sensitive to concentration, as shown in Figures 5 and 6. The formation of the contact ion pairs between NH_4^+ and SO_4^{2-} has little effect on the ν_1-SO_4^{2-} band characteristics. It is interesting to note that the ν_1-SO_4^{2-} band frequency decreases slightly with increasing concentration in supersaturated solutions, which is different from the linear dependence of the band frequency on salt concentration ($\nu_{max} = 980.89 + 0.176C$) in dilute bulk solutions observed by Rudolph et al.[22]

Conclusions

Combining the single-particle levitation technique and in-situ Raman spectroscopy, we have obtained Raman spectra of single $MgSO_4$ solution droplets in highly supersaturated states with a water-to-solute ratio as low as 1.54. We have observed the Raman characteristics of the contact ion pairs between Mg^{2+} and SO_4^{2-}. When the water-to-solute ratio decreases to 8, the ν_1-SO_4^{2-} band shows abrupt changes, which are attributed to the formation of a large number of contact ion pairs with different structures. A chain structure composed of the contact ion pair of bidentate in highly supersaturated $MgSO_4$ solutions was also proposed. The formation of such a chain can explain the observed mass transfer limitation in the evaporation of $MgSO_4$ solutions.

On the basis of the comparisons of the evolution of the Raman spectra of $MgSO_4$ and $(NH_4)_2SO_4$ solutions as the water-to-solute ratio decreases to below 6, we believe that the shoulder usually appearing at 995 cm^{-1} in dilute $MgSO_4$ solutions is related to the contact ion pairs instead of the solvent-separated ion pairs previously reported in some literature. Coupling with Raman spectroscopy, the EDB is a useful tool for studying molecular structures of supersaturated solutions.

Acknowledgment. Financial support of the Hong Kong RGC Earmarked Grant (HKUST 665/96P) and the HKUST PDF Grant is gratefully acknowledged. All experiments were conducted at HKUST.

References and Notes

(1) Pilinis, C.; Seinfeld, J. H.; Grosjean D. *Atmos. Environ.* **1989**, *23*, 1601.
(2) Wexler, A. S.; Seinfeld, J. H. *Atmos. Environ.* **1990**, *24A*, 1231.
(3) Meng, Z.; Seinfeld, J. H. *Atmos. Environ.* **1996**, *30*, 2889.
(4) Andrews, E.; Larson, S. M. *Environ. Sci. Tech*. **1993**, *27*, 857.
(5) Hansson, H.-C.; Rood, M. J.; Koloutsou-Vakakis, S.; Hameri, K.; Orsini, D.; Kawamura, K.; Semere, R.; Imai, Y.; Fujii, Y.; Hayashi, M. *J. Geophys. Res*. **1996**, *101* (D13), 18721.
(6) Shulman, M. L.; Charlson R. J.; Davis, E. J. *J. Aerosol Sci.* **1997**, *28*, 737.
(7) Chan, C. K.; Flagan, R. C.; Seinfeld, J. H. *J. Am. Ceram. Soc*. **1998**, *81*, 646.
(8) Chan, C. K.; Ha, Z.; Choi, M. Y. *Atmos. Environ.* **2000**, *34*, 4795.
(9) Brown, P. G. M.; Prue, J. E. *Proc. R. Soc. A* **1955**, *232*, 320.
(10) Nair, V. S. K.; Nancollas, G. H. *J. Chem. Soc.* **1958**, 3706.
(11) Eigen, M.; Tamm, K. *Z. Elektrochem.* **1962**, *66*, 107.
(12) Atkinson, G.; Pstriucci, S. *J. Phys. Chem*. **1966**, *70*, 3122.
(13) Marshall, W. L. *J. Phys. Chem.* **1967**, *71*, 3584.
(14) Davis, A. R.; Oliver, B. G. *J. Phys. Chem*. **1973**, *77*, 1315.
(15) Chatterjee, R. M.; Adams, W. A.; Davis, A. R. *J. Phys. Chem*. **1974**, *78*, 246.
(16) Pye, C. C.; Rudolph, W. W. *J. Phys. Chem. A* **1998**, *102*, 9933.
(17) Rull, F.; Prieto, M.; Sobron, E. J. *De Physique* **1994**, *IV.4 C2*, 47.
(18) Rull, F. *Z. Naturforsch*. **1995**, *50a*, 292.
(19) Rudolph, W. W.; Schoenher, S. *Z. Phys. Chem.* (*Munich*) **1991**, *31*, 172.
(20) Rudolph, W.; Brooker, M. H.; Tremaine, P. *J. Solution Chem*. **1997**, *26*(*8*), 757.
(21) Rudolph, W. *Ber. Bunsen-Ges. Phys. Chem.* **1998**, *102*, 183.
(22) Rudolph, W.; Irmer, G. *J. Solution Chem.* **1994**, *23*, 663.
(23) Rudolph, W. F.; Pye, C. C. *J. Phys. Chem. B* **1998**, *102*, 3564.
(24) Daly, F. P.; Brown, C. W.; Kester, D. R. *J. Phys. Chem.* **1972**, *76*, 3664.
(25) Rull, F.; Balarew, Ch.; Alvarez, J. L.; Sobron, F.; Rodriguez, A. *J. Raman Spectrosc.* **1994**, *25*, 933.
(26) Davis, E. J. *Aerosol Sci. Technol*. **1997**, *26*, 212.
(27) Tang, I. N.; Fung, K. H.; Imre, D. G.; Munkelwitz, H. R. *Aerosol Sci. Technol*. **1995**, *23*, 443.
(28) Tang, I. N.; Fung, K. H. *J. Chem. Phys*. **1997**, *106*, 1653.
(29) Cohen, M. D.; Flagan, R. C.; Seinfeld, J. H. *J. Phys. Chem.* **1987**, *91*, 4563.
(30) Ha, Z.; Chan, C. K. *Aerosol Sci. Technol.* **1999**, *31*, 154.
(31) Buehler, M. F.; Allen, T. M.; Davis, E. J. *J. Coll. Interface Sci*. **1991**, *146*, 79.
(32) Foss, W.; Li, W.; Allen, T. M.; Blair, D. S.; Davis, E. J. *Aerosol Sci. Technol.* **1993**, *18*, 187.
(33) Rassat, S. D.; Davis E. J. *J. Aerosol Sci.* **1992**, *23*, 165.
(34) Schweiger, G. In *Analytical Chemistry of Aerosols*; Spurny K. R., Ed.; Lewis Publishers, CRC Press: Boca Raton, 1999; pp 319−352.
(35) Nomura, H.; Shinobu, K.; Miyahara, Y. In *Water Metal Cations in Biological System*, Proc. Symp. 1978; Pullman B., Yaji, K., Eds.; Japan Sci. Soc. Press: Tokyo, 1980; pp 31−46.
(36) Hayes, A. C.; Kruus, P.; Adams, W. A. *J. Solution Chem*. **1984**, *13*, 61.
(37) Rull, R.; Frantz, J. D.; Dubessy, J. In *Proceedings of the 4th International Symposium on Hydrothermal Reactions*; Cuney, M., Cathalineau, M., Eds.; Institut Lorraine des Geosciences: Nancy, 1993; pp 213−215.
(38) Nakamoto, K.; Fujuta, J.; Tanaka, S.; Kobayashi, M. *J. Am. Chem. Soc.* **1957**, *79*, 4904.
(39) Barraclough, C. G.; Tobe, M. L. *J. Chem. Soc*. **1961**, 1993.
(40) Eskenazi, R.; Rasovan, J.; Levitus, R. J. *Inorg. Nucl. Chem.* **1966**, *28*, 521.
(41) Finholt, J. E.; Anderson, R. W.; Fyfe, J. A.; Caulton, K. G. *Inorg. Chem.* **1965**, *4*, 43.
(42) Horn, R. W.; Weissberger, E.; Collman, J. P. *Inorg. Chem.* **1970**, *9*, 2367.
(43) Matwiyoff, N. M.; Taube, H. *J. Am. Chem. Soc*. **1968**, *90*, 2796.
(44) Caminiti, R.; Licheri, G.; Piccaluga, G. *J. Appl. Crystallogr*. **1972**, *12*, 34.
(45) Fran, H. S.; Wen, W. Y. *Discuss. Faraday Soc*. **1957**, *24*, 133.